



# Taguchi Design of Experiment (DoE) for Evaluating TIG-welding Parameter Variations on Tensile-shear Load and Hardness Using Stainless Steel 304 Material

Taguchi Design of Experiment (DoE) untuk Mengevaluasi Variasi Parameter Pengelasan TIG pada Beban Tarik-Geser dan Kekerasan Menggunakan Material SUS 304

Siswanto<sup>1</sup>, Sukarman<sup>1\*</sup>, Dodi Mulyadi<sup>1</sup>, Amir<sup>1</sup>, Amri Abdulah<sup>2</sup>, Ean Deka Putra<sup>2</sup>

<sup>1</sup>Department of mechanical engineering, Faculty of engineering, Universitas Buana Perjuangan Karawang, 41361, Indonesia

<sup>2</sup>Department of mechanical engineering, STT Wastukencana, Purwakarta, 41151, Indonesia

## Article information:

Received:  
19/04/2024  
Revised:  
01/05/2024  
Accepted:  
03/05/2024

## Abstract

This article delves into the intricacies of optimizing the TIG welding process using stainless steel 304 (SUS 304) material, with particular emphasis on small-scale industries that are heavily reliant on TIG welding, especially in the production of household equipment and fences. The objective of this research is to enhance the tensile shear load (T's load) through the Taguchi Design of Experiment (DoE), which takes into account welding current, gas flow rate, and electrode diameter as primary parameters. This study evaluates T's load and hardness across the welding zone, which includes the heat-affected zone (HAZ) and base metal. The study was conducted using a Stahlweld inverter welding machine operating at 220 V/50 Hz, and a maximum T's load of 1545.1 kgf was achieved in the fourth iteration. The optimization of T's load was carried out using SN ratio analysis and involved setting the welding current to level II, gas flow rate to level I, and electrode diameter to level II following the Taguchi DoE design. The hardness peaks in the weld area decreased in the HAZ and reached their lowest point in the base metal. These findings provide valuable insights into optimizing TIG welding parameters for thin stainless steel 304 materials, which supports Sustainable Development Goal 9 (industry, innovation, and infrastructure).

**Keywords:** design of experiment (doe), Taguchi design, sus 304, tig-welding, tensile-shear load.

## SDGs:



## Abstrak

Artikel ini mendalami seluk-beluk optimalisasi proses pengelasan TIG dengan menggunakan material stainless steel 304 (SUS 304), dengan penekanan khusus pada industri skala kecil yang sangat bergantung pada pengelasan TIG, khususnya pada produksi peralatan rumah tangga dan pagar. Penelitian ini bertujuan untuk meningkatkan beban geser tarik (beban T) melalui Taguchi Design of Experiment (DoE) yang memperhitungkan arus pengelasan, laju aliran gas, dan diameter elektroda sebagai parameter utama. Studi ini mengevaluasi beban dan kekerasan T di seluruh zona pengelasan, yang meliputi zona yang terkena dampak panas (HAZ) dan logam dasar. Penelitian dilakukan dengan menggunakan mesin las inverter Stahlweld yang beroperasi pada tegangan 220 V/50 Hz, dan diperoleh beban T maksimum sebesar 1545,1 kgf pada iterasi keempat. Optimalisasi beban T dilakukan dengan menggunakan analisis rasio SN dan melibatkan pengaturan arus pengelasan ke level II, laju aliran gas ke level I, dan diameter elektroda ke level II mengikuti desain Taguchi DoE. Puncak kekerasan pada daerah las mengalami penurunan pada HAZ dan mencapai titik terendah pada logam dasar. Temuan ini memberikan wawasan berharga dalam mengoptimalkan parameter pengelasan TIG untuk material baja tahan karat tipis 304, yang mendukung Tujuan Pembangunan Berkelanjutan 9 (industri, inovasi, dan infrastruktur).

**Kata Kunci:** design of experiment (doe), taguchi design, sus 304, tig-welding, tensile-shear load.

\*Correspondence Author  
email : [sukarman@ubpkarawang.ac.id](mailto:sukarman@ubpkarawang.ac.id)



This work is licensed under a [Creative Commons Attribution-NonCommercial 4.0 International License](https://creativecommons.org/licenses/by-nc/4.0/)

## 1. INTRODUCTION

This research endeavours to improve the quality of tungsten inert gas welding (TIG welding), particularly concerning its application in small-scale industries such as household equipment and fencing. These industries heavily rely on stainless steel 304 (SUS 304) for their manufacturing processes. However, challenges arise, especially when welding thin materials, necessitating optimization strategies to enhance weld quality and strength. A common issue is inadequate fusion or penetration during thin SUS 304 materials welding, resulting in weaker weld joints with compromised mechanical integrity (Xie *et al.*, 2018). Furthermore, thin materials are prone to distortion and warping during welding, leading to irregular welds and workpiece deformation.

Additionally, improper control of welding parameters like welding current, gas flow rate, and electrode diameter can result in excessive spatter (Vimal, Vinodh and Raja, 2017), porosity (Wirajaya, Nugroho and Suwasono, 2021), or weld cracking (Datta *et al.*, 2002), further diminishing weld quality and structural reliability (Venkatesan, Muthupandi and Justine, 2017). Addressing these welding challenges is crucial, as weak welds can lead to product defects, increased damage rates, and reduced overall performance and reliability of welded components (Singh and Vijayakumar, 2012; Wu *et al.*, 2019). Hence, optimizing TIG welding parameters for thin SUS 304 materials is important for these industries. Figure 1 provides an illustrative example of TIG-welding's application in this study.



Figure 1. TIG-welding application on pan handles (Media, 2018).

Numerous studies within the modern industry of TIG-welding highlight efforts by researchers to optimize TIG-welding process parameters, employing robotic technology to enhance welding precision across various steel types (Reddy and VenkataRamana, 2018). Ahmad and Alam, employed Taguchi DoE design to optimize TIG-welding parameters, aiming to enhance joint quality (Ahmad and Alam, 2019). Samiuddin *et al.*, explored TIG-welding parameters on aluminum alloys through mechanical and microstructural characterization (Samiuddin *et al.*, 2021). Meanwhile, Nurisna and Setiawan, assessed filler effects in TIG-welding between carbon steel and 316L stainless steel, focusing on their impact on mechanical properties (Nurisna and Setiawan, 2020). Widianto, *et al.*, investigated mechanical properties, welding positions, and characteristics of Orbital Pulse Current Gas Tungsten Arc Welding (PC-GTAW) on AISI 304L stainless steel pipes, utilizing TIG technology (Widianto, Baskoro and Kiswanto, 2022). Shrivastava *et al.*, explored TIG-welding parameters to enhance weld strength (Shrivastava *et al.*, 2020). Sirohi *et al.*, investigated autonomous TIG-welding methods on Alloy 617 and AISI 304H steel for Advanced Ultra-Supercritical (AUSC) applications, emphasizing mechanical properties and microstructure (Sirohi *et al.*, 2023). In a separate investigation, Amar *et al.*, delved into TIG welding parameters to address direct tensile load (DT-load) on different steel thicknesses, utilizing SPCC-SD materials of varying thicknesses in the experimental setup (Amar *et al.*, 2024). Their research elucidated improvements in weld quality specifically tailored for DT-load conditions (Amar *et al.*, 2024).

Despite the extensive research on TIG-welding, there remains a need for explicit investigation into various TIG-welding parameters and their effects on the T's loads and hardness of SUS 304 material. This study delves into the impacts of modifying input parameters using the Taguchi Design of Experiment (DoE) design, employing three parameters at three experimental levels: welding current, gas flow rate, and tungsten diameter. The specific focus on welding thin stainless-steel materials is expected to significantly impact industries, particularly those involved in manufacturing

stainless steel components for household appliances. The research objective is to enhance understanding of how TIG-welding parameters, such as current, voltage, and electrode diameter, influence the T's loads of SUS 304 material. This study provides crucial insights for improving the manufacturing process of durable household appliances and ensuring their future reliability.

## 2. METHODOLOGY

### 2.1. Material

The selection of SUS 304 material, which has a thickness of 1 mm, was primarily motivated by its exceptional corrosion resistance properties. These properties make it a preferred choice for applications within the food industry and household utensils. Considering the rigorous demands for food-grade materials, utilising such materials becomes imperative. The chemical composition of SUS 304 material, as per the JIS G 4305 standard, includes carbon (C)  $\leq 0.08\%$ , silicon (Si)  $\leq 1.00\%$ , manganese (Mn)  $\leq 2.00\%$ , phosphorus (P)  $\leq 0.045\%$ , sulphur (S)  $\leq 0.030\%$ , nickel (Ni) within a range of 8.00-10.50%, and chromium (Cr) within a range of 18.00-20.00% (ANSI, 2012). Meanwhile, the mechanical properties of SUS 304 material comply with the JIS G 4305 standard, as detailed in Table 1 (ANSI, 2012).

**Table 1.** The mechanical properties of SUS 304.

Specification	Proof stress (N/mm <sup>2</sup> )	T's loads (N/mm <sup>2</sup> )	Elongation (%)
JIS G 4305	$\geq 205$	$\geq 520$	$\geq 40$
Test Report	210	540	42

TIG welding operations utilize WT20 tungsten electrodes conforming to the ANSI/AWS A5.12M-98 and ISO 6848 standards (AWS, 1998). These electrodes, produced by Luoyang Jiangchi Metal Material Co., Ltd., are available in sizes of 1.6, 2.4, and 3.2 mm, akin to SUS 304 materials, and are readily accessible in the market, as noted by Singh and Vijayakumar (Singh and Vijayakumar, 2012). The composition of these tungsten electrodes complies with AWS A5.5 class EWTH-2 specifications, incorporating thorium dioxide (ThO<sub>2</sub>) in ranges of 1.70% to 2.20% (ANSI/AWS, 1998). Material preparation involves employing a

Q01-1.5x1320 (52\*) foot shear machine at the Karawang UBP Laboratory for the shearing process, with the cutting force determined by equation (1), as reported by (Krininger et al., 2017):

$$F_s = R_m \cdot S \cdot L \quad (1)$$

Where  $F_s$  is donated for the force shearing minimum (N),  $R_m$  is donated for T's loads (MPa) and  $L$  is donated for the length of the material to be sheared (mm).

### 2.2. Tensile Load Test and Welding Desain

The TIG-welding is widely used in various sectors like construction, aerospace, automotive, and more to join metal components (Wu et al., 2019). During TIG-welding, T's loads analysis evaluates welded joint strength and integrity under tensile and shear loads (Venkatesan, Muthupandi and Justine, 2017). This analysis is crucial for assessing weld joint quality by testing their resistance to tension force (Amar et al., 2024) and shear force (Sukarman, Triyono, et al., 2023). Engineers and welders rely on T's loads analysis to ensure welded joints meet performance and strength standards, enhancing overall reliability and safety. T's loads testing aims to assess material strength under compression and tension forces and identify failure modes post-testing.

The TIG-welding design suggests adding extra support plates to welded joints for better strength. Also, pressure plate joints must be adjusted to meet standards. The connection design is detailed in Figure 2. This design involves welding a support plate to the main plate using a 10.0 mm drilled hole. Figure 2 shows this connection design and how data is collected for research samples. The Hung Ta HT-9102 50 kN, 380 Volt universal testing machine will test the samples at 40 mm/minute, as shown in Figure 2. The machine is calibrated in kilograms-force (.kgf). The stainless steel follows the JIS G 4305 reference standard and is cut precisely according Figure 2's design (ASME, 2023).

T's loads testing not only determines a material's strength and resistance to T's loads but also identifies post-test failure modes.

Among these failure modes are pullout failures, involving the removal of one material from another, and interfacial failures, involving the separation of two interconnected materials (Ghazali *et al.*, 2019; Shrivastava *et al.*, 2020). Interfacial failure occurs when there is detachment between related materials, such as layers of material, or between a base material and additional layers (Jeong *et al.*, 2017; Das, Das and Paul, 2020). On the other hand, pullout failure modes are crucial for understanding the strength of material bonds and their ability to withstand forces before separation occurs (Heydari and Akbari, 2020).

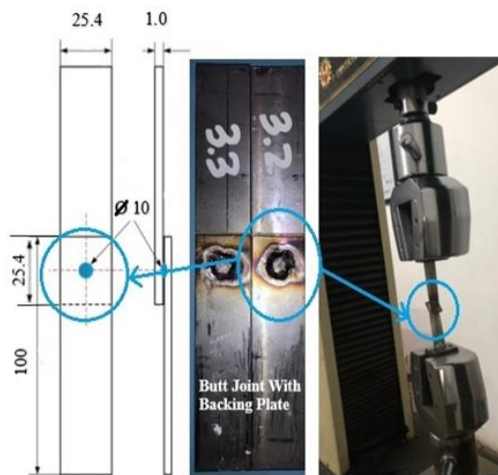


Figure 2. T's loads testing and TIG-welding design (all dimensions in mm).

### 2.3. TIG-welding Parameters and Taguchi DoE Design

Several experimental studies have utilized the Taguchi DoE design approach for process optimization, spanning various welding processes such as resistance spot welding (Sukarman and Abdulah, 2020; Sukarman, Abdulah, *et al.*, 2021), laser welding (Uijl *et al.*, 2012), friction stir welding (Armansyah and Chie, 2018), TIG-welding (Kobayashi *et al.*, 2004; Ragavendran *et al.*, 2017). Additionally, the effectiveness of the DOE TAGUCHI DESIGN method was chosen and demonstrated in optimizing research areas such as bio-jet oil (Siswanto *et al.*, 2022), building concrete (Prabha *et al.*, 2021), machining processes (Khoirudin *et al.*, 2023), metal forming (Sukarman *et al.*, 2020) and painting application (Sukarman, Shieddieque, *et al.*, 2021).

The adoption of Taguchi DoE design in this study is based on prior research and aims to examine how variations in input parameters impact the T's loads of SUS 304 material during TIG-welding. The controlled parameters used are listed in Table 2. The Stahlweld TIG 160 welding inverter is selected and configured to operate at a voltage of 220 V with a frequency of 50 Hz. It provides a current range of approximately 10 to 160 amperes. Welders possessing a minimum of 5G certification are required to execute the welding procedure in strict adherence to safety protocols. The chosen input variables comprise the flow rate of argon gas, the electric current, and the diameter of the tungsten electrode. The T's loads test sample is repeated thrice at each level, resulting in 24 samples, as illustrated in Figure 3. The objective is to regulate input parameters using the Taguchi DoE design approach, employing statistical software specified in Table 3.

### 2.4. Signal to Noise Ratio (SN-Ratio)

In welding applications, the Signal-to-Noise Ratio (SN-Ratio) serves as a measure comparing the strength of the desired welding signal to the unwanted noise within the welding process or equipment (Muthu, 2019; Sukarman, Khoirudin, *et al.*, 2023). SNR is used to assess the quality of response data (Sukarman and Abdulah, 2020). The SNR characteristics are typically categorized into three data characteristics as illustrated in equations (2)-(4) (Montgomery, 2010):  
Smaller is better:

$$SN-Ratio = -10 \log \sum_{i=1}^{n_0} \frac{y_i^2}{n_0} \quad (2)$$

Larger is better:

$$SN-Ratio = -10 \log \frac{1}{n_0} \sum_{i=1}^{n_0} \frac{1}{y_i^2} \quad (3)$$

Nominal is the best:

$$SN-Ratio = -10 \log \frac{\bar{y}^2}{s^2} \quad (4)$$

Where n denoted for the number of samples, y is the response parameters,  $\bar{y}$  denoted for the average of the responding factor, and s is the variant of the response variable. By analyzing experimental results and conducting surface response analysis, the correlation between

Table 2. The Taguchi DoE design parameters.

Code	TIG-Welding Parameter	Units	Level Experiment	
			LI	LII
A	Welding current, <i>I</i>	A, ampere	50	60
B	Gas Flow rate, <i>V<sub>g</sub></i>	LPM	12	18
C	Electrode Diameter, <i>D<sub>e</sub></i>	mm	1.6	3.2

Table 3. TIG-welding sample DoE Taguchi design parameters and identifications.

Run No	Welding Current, (A)	Gas Flow Rate, (LPM)	Electrode Diameter, (mm)	Sample Identification		
				TS Loads 1	TS Loads 2	TS Loads 3
1	50	12	1.6	S-1.1	S-1.2	S-1.3
2	50	12	3.2	S-2.1	S-2.2	S-2.3
3	50	18	1.6	S-3.1	S-3.2	S-3.3
4	50	18	3.2	S-4.1	S-4.2	S-4.3
5	60	12	1.6	S-5.1	S-5.2	S-5.3
6	60	12	3.2	S-6.1	S-6.2	S-6.3
7	60	18	1.6	S-7.1	S-7.2	S-7.3
8	60	18	3.2	S-8.1	S-8.2	S-8.3



Figure 3. TIG-welding coupon: 24-unit sample from 8 iterations of SUS 304 steel sheets.

process variables and the measured response becomes evident. This understanding helps in identifying the optimal conditions to achieve the desired T's load in TIG-welding results.

### 2.5. The Evaluation of Hardness in the Welding and Heat-Affected Zones

The AR936 portable hardness tester assesses hardness by traversing the welding area, Heat-Affected Zone (HAZ), and non-HAZ regions at 2.5 mm intervals. It begins from the center of distinct HAZ regions within the circle.

The welding area is positioned around 5 mm radially from the circle's center. Conversely, the HAZ spans from 8 to 10 mm and from 0 to 2 mm from the circle's center.

Figure 4 provides a comprehensive depiction of the welding site and the hardness measurement instrument, including specific details.

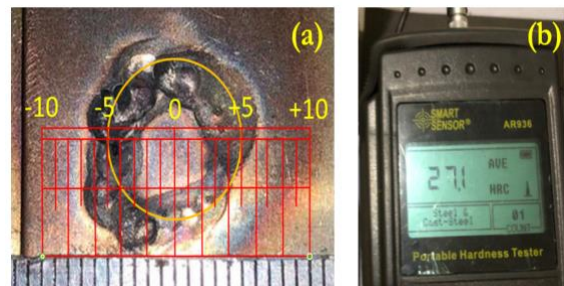


Figure 4. Hardness test of TIG-welding samples; (a) Hardness area of measurement; (b) Visual hardness tester.

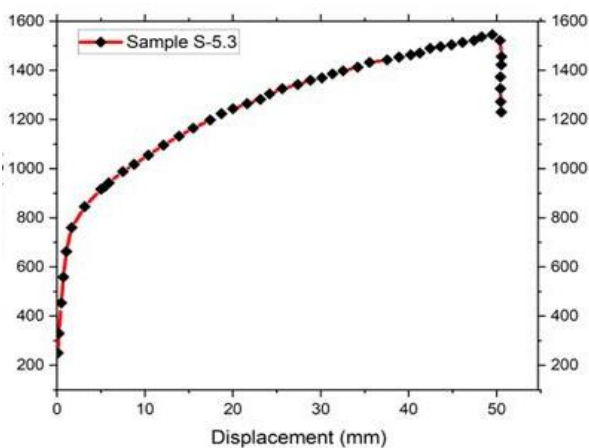
### 3. RESULTS AND DISCUSSION

#### 3.1. T's Loads Analysis

The presented test results in Table 4 reveal significant variations in welding process performance across various parameter combinations. Notably, welding currents of 50 A and 60 A exhibit distinct average T's loads outcomes, with the highest observed in run four at 60 A. Similarly, gas flow rates of 12 LPM and 18 LPM display differing mean T's loads, with the lowest average T's loads observed in run four at 18 LPM. Electrode diameters of 1.6 mm and 3.2 mm also contribute to T's loads variation across iterations, with the fifth run showcasing the highest average stress test load. Remarkably, while the fifth run exhibits the highest average T's loads, the peak T's loads occur during the third sample iteration, specifically with sample code S-5.3. This occurrence is attributed to welding current parameters of 60 A, a gas flow rate of 12 LPM, and an electrode diameter of 3.2 mm.



(a) Observations of pullout failure mode



(b) Identification of the highest T's loads in Run No. S-5.3

Figure 5. T's loads evaluation includes the following aspects.

Figure 5a visually depicts the pullout failure mode observed during T's loads testing, indicative of material extraction or separation from the

welded joint. This failure mode, commonly encountered in welding evaluations and specifically addressed in TIG-welding tests conducted in this research, underscores the need for meticulous parameter optimization to ensure structural integrity and weld quality as reported by Al-Sabur and Heydari & Akbari (Heydari and Akbari, 2020; Al-Sabur, 2021). The T's loads analysis assesses the influence of input parameters on T's loads, as outlined in Table 4 for SUS 304 using TIG welding. It is noteworthy that iteration S-5.3 achieves a maximum T's loads of 1545.1 kgf, highlighting the effectiveness of the specific parameter configurations used. These experiments entailed methodical manipulation of variables to reveal crucial insights. In this work, the welding current was fixed at 60A, the gas flow rate was set to 12 LPM, and the electrode diameter was 1.6 mm.

#### 3.2. SN-ratio Analysis and Predictions

T's load data characteristics from the TIG-welding test results indicate a preference for larger values (Larger is better), suggesting that higher T's load values correlate with better quality TIG-welding outcomes (Sukarman, Khoirudin, et al., 2023; Amar et al., 2024). Consequently, Equation (3) is employed in the signal-to-noise ratio (SNR) analysis, with the results outlined in Figure 6. Multiple linear regressions were performed using statistical software to predict the SN ratio. The linear regression equation incorporates three variables: A represents welding current, B indicates gas flow rate, and C signifies electrode diameter. Thus, Equation (5) is the linear regression model illustrating the SN-ratio. Figure 6 SN-ratio analysis indicates a direct proportionality between welding current and electrode diameter with T's loads. Higher values of welding current and electrode diameter lead to better T's loads performance, a finding supported by Amar et al. (Amar et al., 2024):

$$SNR_{-pred.} = 53.08 + 0.002494A + 0.002041B + 0.002437C \quad (5)$$

The optimal T-S load condition is attained by setting welding current, gas flow rate, and electrode diameter parameters at the 2nd level, 1st level, and 2nd level, respectively.

Table 4. T's loads experiment result and visual examinations.

Run No	Welding Current, (A)	Gas Flow Rate, (LPM)	Electrode Diameter, (mm)	TS Loads 1	TS Loads 2	TS Loads 3	T's loads, Ave.	SN Ratio		Failure Mode Analysis
								Experimental	Prediction	
1	50	12	1.6	1322.2	1061.8	1192.3	1192.1	61.42	61.45	Pull out
2	50	12	3.2	1326.8	1191.3	1448.3	1322.1	62.34	62.04	Pull out
3	50	18	1.6	1162.0	1069.1	920.2	1050.4	60.31	60.72	Pull out
4	50	18	3.2	1435.4	1526.9	1300.0	1420.8	62.99	63.24	Pull out
5	60	12	1.6	1475.4	1533.0	1545.1	1576.4	63.62	64.09	Pull out
6	60	12	3.2	1315.2	1418.9	1207.5	1313.9	62.31	62.46	Pull out
7	60	18	1.6	1252.2	1136.9	1304.2	1231.1	61.76	61.52	Pull out
8	60	18	3.2	1360.8	1175.5	1090.4	1208.9	61.54	61.82	Pull out

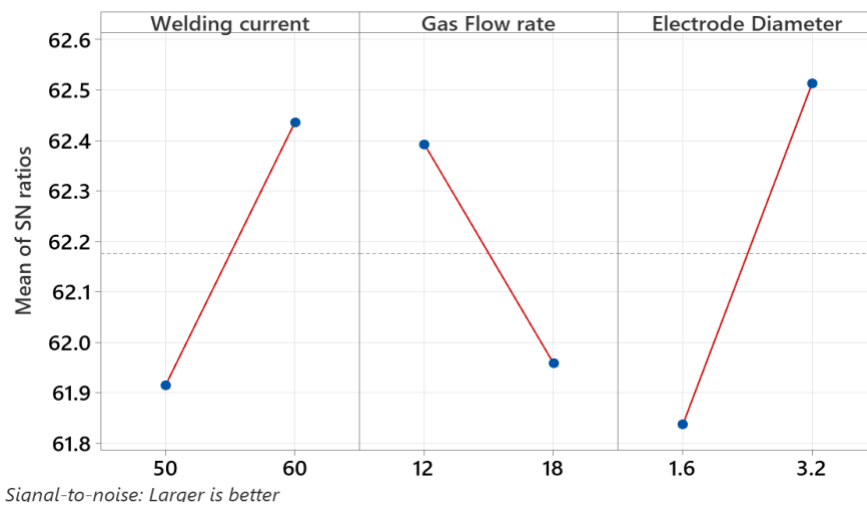


Figure 6. SN-ratio analysis of T's loads in SUS 304 TIG-welding.

Table 5. ANOVA statistical linear model.

Parameter Input	DF	Adj. SS	Adj. MS	F-Value	P-Value	% Contributions
Welding current	1	262.09	262.09	0.39	0.643	59%
Gas flow rate	1	72.81	72.81	0.11	0.796	17%
Electrode diameter	1	106.19	106.19	0.16	0.758	24%

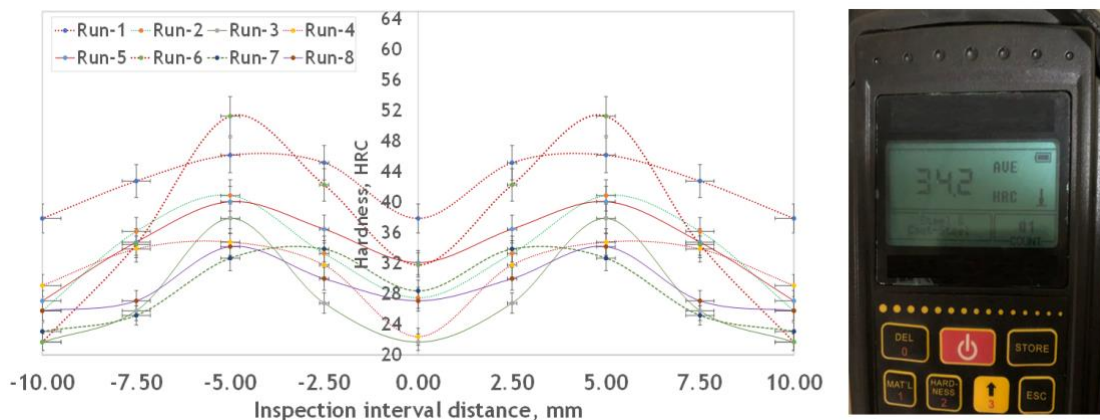


Figure 7. The hardness result examination of TIG-welding SUS 304 material.

The SN ratio prediction using Equation 5 yields precise results, with the deviation below 10% and the actual average condition being approximately 0.11%, peaking at 0.6%. These findings demonstrate a higher accuracy level than the earlier research by Sukarman et. al (Sukarman, Khoirudin, et al., 2023), which reported results of around 7%. This result is also more accurate compared to the 13.92% reported by Singh dan Vijayakumar (Singh and Vijayakumar, 2012) and 10% reported by Wu et al. (Wu et al., 2019).

### 3.3. ANOVA Evaluations

An ANOVA was employed to determine the welding parameters that had a noteworthy impact on the mean T's loads in this welding study. The study findings indicate that the welding current significantly influences the outcomes, with substantial variations observed among the groups using currents of 50 A, and 60 A. Conversely, fluctuations in gas flow remain close to the average T's loads mean. The parameter of electrode diameter demonstrates that variations in the dimensions of the tungsten (1.6 mm and 3.2 mm) significantly impact the average T's loads. Due to the criticality of the results in ensuring weld quality, they can assist in determining the optimal welding parameters. The analysis of variance (ANOVA) results is displayed in Table 5. Further investigation or larger-scale experiments may be necessary to fully understand the interconnectedness of these variables and improve the parameters of the welding process. Two input parameters that notably impact the T's loads are welding current and electrode diameter, as indicated by the ANOVA. Approximately 59% of the overall parameters are influenced by welding current, followed by electrode diameter at about 24%. Similar findings were observed in previous research conducted by Amar et al. (Amar et al., 2024).

### 3.4. Hardness Analysis

Hardness evaluation aims to assess how TIG-welding process parameters affect material hardness, influenced by the heat generated during welding. Hardness testing is carried out to assess the welding effects on various regions, including

the heat-affected zone (HAZ), welding location, and base metal (Endramawan and Sifa, 2018). The hardness evaluation is essential for understanding the impact of welding on different regions such as the heat-affected zone (HAZ), the welding location, and the base metal. Figure 7 shows hardness measurements from nine points across thirteen samples welded using TIG-welding. The 6th iteration reached its peak hardness around 51.3 HRC at positions +5 mm and -5 mm. Results from each iteration reveal that areas with the highest hardness are typically at distances of +5 mm and -5 mm from the centerlines.

The hardness test results indicate that increasing welding current raises HRC at specific locations. However, the relationship between gas flow rate and electrode diameter shows no discernible pattern. Throughout the welding process, variations in hardness are observed. The base metal experiences reduced hardness as it transitions into the heat-affected zone (HAZ). Similar phenomena were noted in previous studies as reported by Sirohi et al. (Sirohi et al., 2023). The highest levels of hardness occur in the -5 and +5 distance areas. This is primarily due to these areas being within the TIG-welding zone, which receives the most intense heating, as reported by Nurisna & Setiawan and Sirohi et al. (Nurisna and Setiawan, 2020; Sirohi et al., 2023).

### 3.5. Statistical Validations

Statistical validation is necessary to determine the three variables that affect the T's loads of SUS 304 steel after TIG-welding. To examine the correlation between all parameters, we employ Equation (6) and the Pearson correlation method (Kotlu and Deshpande, 2018):

$$r = \frac{n(\sum xy) - (\sum x)(\sum y)}{\sqrt{[n\sum x^2 - (\sum x)^2][n\sum y^2 - (\sum y)^2]}} \quad (6)$$

Where n is the number of data pairs, x is the value of the first variable, and y is the value of the second variable.  $\sum xy$  is the sum of the results of multiplying each pair of data x and y. of all values of the second variable.  $\sum x^2$  is the sum of the squares of each value of the first variable, and  $\sum y^2$  is the sum of the squares of each value of the second variable.

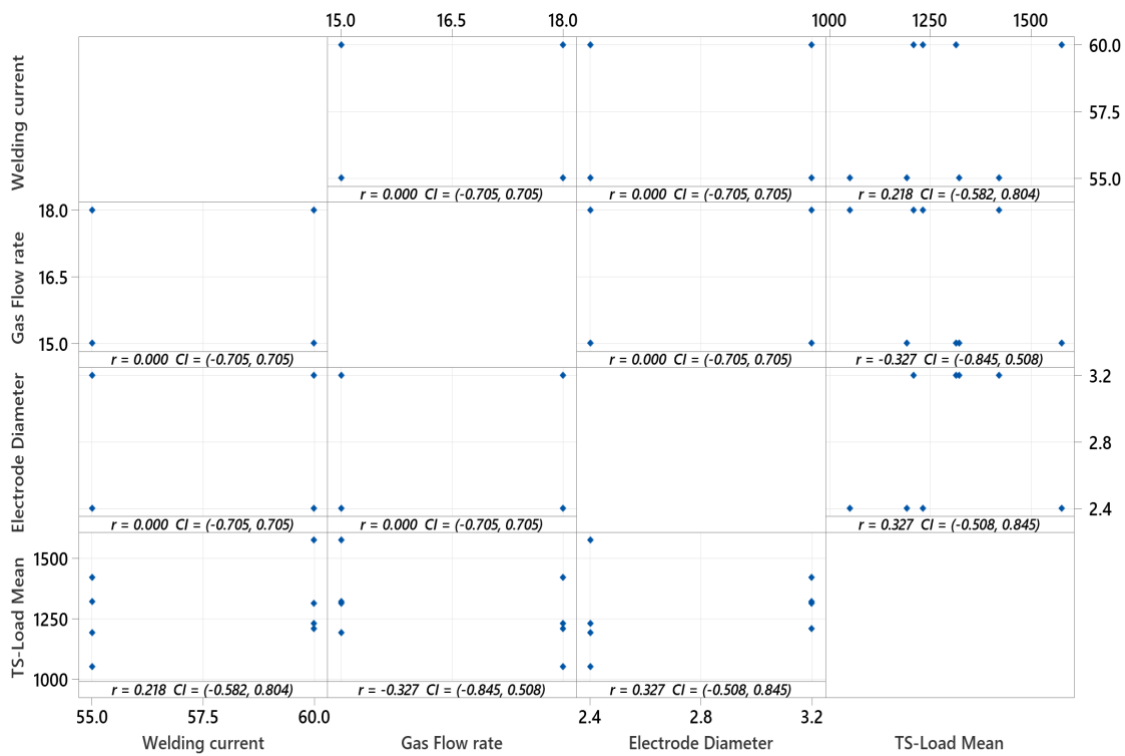


Figure 8. Pearson correlation of TIG-welding parameter with T's loads.

Figure 8 shows the Pearson correlation between T's loads and TIG-welding parameters. This correlation coefficient quantifies the strength and direction of the relationship between continuous variables. For instance, the positive correlation between T's loads, electric current, and electrode diameter in TIG-welding is indicated by Pearson correlation coefficients of approximately 0.218 and 0.327, respectively.

Conversely, the correlation between T's loads and gas flow rate is negative, with a coefficient of around -0.327. A high positive correlation, nearing 1, suggests that T's loads increase with TIG-welding parameters (Nettleton, 2014). On the contrary, a correlation close to -1 implies an inverse relationship.

#### 4. CONCLUSION

The effectiveness of TIG welding on tailless steel SUS 304 can vary based on combinations of parameters like electrode diameter, gas flow rate, and welding current. An evaluation was conducted to assess their impact on weld strength, explicitly focusing on T's loads. Using a gas flow rate of 12 LPM, an electrode diameter of

1.6 mm, and a welding current of 60 A, the highest recorded T's loads was 1545 kgf. Based on SN-ratio analysis and DoE Taguchi design, the optimum T's loads occurred at a welding current of 60A, gas flow rate of 12 LPM, and electrode diameter of 3.2 mm. Statistical analysis via ANOVA revealed that welding current and electrode diameter of TIG-welding parameters have significantly influenced outcomes, while gas flow rate fluctuations had minimal effects. The T's loads data exhibited a normal distribution pattern, enabling appropriate statistical techniques. Hardness tests indicated increased hardness with higher welding currents, although gas flow rate and electrode diameter impacts were inconsistent. Further recommendations include a comprehensive examination and rigorous statistical analysis, considering additional variables like welding materials and environmental conditions to validate results. The hardness analysis results indicate that the welding area exhibits the highest hardness in comparison to other areas, while the base metal demonstrates the lowest hardness.

## ACKNOWLEDGMENTS

The author extends his most profound gratitude and appreciation to the LAB Team of Universitas Buana Perjuangan Karawang for their invaluable support, provision of necessary resources, and creation of a conducive environment essential for the successful completion of this project.

## REFERENCES

- Ahmad, A. and Alam, S. (2019) 'Parametric Optimization Of TIG Welding Using Response Surface Methodology', in *Materials Today: Proceedings. 9th International Conference of Materials Processing and Characterization, ICMP-2019*, Andhra Pradesh, India: Gokaraju Rangaraju Institute Of Engineering and Technology (9th International Conference of Materials Processing and Characterization, ICMP-2019), pp. 3071-3079.
- Al-Sabur, R. (2021) 'Tensile Strength Prediction Of Aluminium Alloys Welded By FSW Using Response Surface Methodology - Comparative Review', in *Materials Today: Proceedings. Second International Conference on Aspects of Materials Science and Engineering (ICAMSE 2021)*, Chandigarh, India: Panjab University (Second International Conference on Aspects of Materials Science and Engineering (ICAMSE 2021)), pp. 4504-4510.
- Amar et al. (2024) 'Enhancing TIG Welding Parameters For Direct Tensile Load (DT-load) On Various Steel Thicknesses', *Jurnal Polimesin*, 22(1), pp. 112-119.
- ANSI (2012) 'JIS G 4305:2012 - Cold-rolled stainless steel plate, sheet and strip'. ANSI. Available at: <https://webstore.ansi.org/standards/jis/jis43052012> (Accessed: 13 July 2023).
- Armansyah and Chie, H.H. (2018) 'Optimization of Process Parameters on Tensile Shear Load of Friction Stir Spot Welded Aluminum Alloy (Aa5052-H112)', *SINERGI*, 22(3), pp. 185-192.
- ASME (2023) *BPVC Section II-Materials Part C-Specifications for Welding Rods, Electrodes & Filler Metals - Specification for titanium and titanium-alloy welding electrodes and rods*. Available at: <https://www.asme.org/codes-standards/find-codes-standards/bpvc-iic-bpvc-section-ii-materials-part-c-specifications-welding-rods-electrodes-filler-metals/2023/print-book> (Accessed: 11 July 2023).
- AWS (1998) 'AWS A5.12/A5.12M-98 (R2007) - Specification for Tungsten and Tungsten-Alloy Electrodes for Arc Welding and Cutting'. Available at: <https://webstore.ansi.org/standards/aws/awsa51212m98r2007> (Accessed: 11 June 2023).
- Das, T., Das, R. and Paul, J. (2020) 'Resistance Spot Welding Of Dissimilar AISI-1008 Steel/Al-1100 Alloy Lap Joints With A Graphene Interlayer', *Journal of Manufacturing Processes*, 53, pp. 260-274.
- Datta, R. et al. (2002) 'Weldability Characteristics Of Shielded Metal Arc Welded High Strength Quenched And Tempered Plates', *Journal of Materials Engineering and Performance*, 11(1), pp. 5-10.
- Endramawan, T. and Sifa, A. (2018) 'Non Destructive Test Dye Penetrant and Ultrasonic on Welding SMAW Butt Joint with Acceptance Criteria ASME Standard', in *IOP Conference Series: Materials Science and Engineering. 2nd International Conference on Innovation in Engineering and Vocational Education*, Manado, Indonesia: Universitas Pendidikan Indonesia, p. 012122.
- Ghazali, F.A. et al. (2019) 'Three Response Optimization of Spot-Welded Joint Using Taguchi Design and Response Surface Methodology Techniques', in M. Awang (ed.) *The Advances in Joining Technology*. Singapore: Springer, pp. 85-95.
- Heydari, H. and Akbari, M. (2020) 'Investigating The Effect Of Process Parameters On The Temperature Field And Mechanical Properties In Pulsed Laser Welding Of Ti6Al4V Alloy Sheet Using Response Surface Methodology', *Infrared Physics & Technology*, 106, p. 103267.
- Jeong, H. et al. (2017) 'Numerical Analysis Of Weld Pool For Galvanized Steel With Lap Joint In GTAW', *Journal of Mechanical Science and Technology*, 31(6), pp. 2975-2983.
- Khoirudin et al. (2023) 'Optimization of S-EDM Process Parameters on Material Removal Rate using Copper Electrodes', *Jurnal Polimesin*, 21(1), pp. 17-20.
- Kobayashi, K. et al. (2004) 'Practical Application of High Efficiency Twin-Arc TIG Welding Method (Sedar-TIG) for PCLNG Storage Tank', *Welding in the World*, 48(7), pp. 35-39.
- Kotu, V. and Deshpande, B. (2018) 'Chapter 4: Classification', in *Data Science: Concepts and Practice*. USA: Morgan Kaufmann, pp. 65-163.
- Krinninger, M. et al. (2017) 'On the Influence of Different Parameters on the Characteristic Cutting Surface when Shear Cutting Aluminum', in *Procedia CIRP. Manufacturing Systems 4.0 - Proceedings of the 50th CIRP Conference on*

- Manufacturing Systems* (Manufacturing Systems 4.0 - Proceedings of the 50th CIRP Conference on Manufacturing Systems), pp. 230-235.
- Media, P.K.C. (2018) *Industri Penggorengan Raksasa Asal 'Gang Dag Deg Dog' Bandung Tembus Pasar Luar Negeri*. Available at: <https://www.kompasiana.com/dennysuryadharm/5a9ab7bfdd0fa8392b414872/penggorengan-raksasa-asal-gang-dag-deg-dog-bandung> (Accessed: 12 March 2023).
- Montgomery, D.C. (2010) *Design and Analysis of Experiments, Minitab Manual*. 7th edn. USA: John Wiley & Sons. [Print].
- Muthu, P. (2019) 'Optimization of the Process Parameters of Resistance Spot Welding of AISI 316L Sheets Using Taguchi Method', *Mechanics and Mechanical Engineering*, 23, pp. 64-69.
- Nettleton, D. (2014) 'Chapter 6 - Selection of Variables and Factor Derivation', in D. Nettleton (ed.) *Commercial Data Mining*. Boston: Morgan Kaufmann, pp. 79-104.
- Nurisna, Z. and Setiawan, E. (2020) 'Pengaruh Filler Pada Pengelasan Tig Baja Karbon dan Stainless Steel 316L Terhadap Sifat Mekanik', *Quantum Teknika : Jurnal Teknik Mesin Terapan*, 1(2), pp. 95-99.
- Prabha, S. et al. (2021) 'Plant-Derived Silica Nanoparticles And Composites For Biosensors, Bioimaging, Drug Delivery And Supercapacitors: A Review', *Environmental Chemistry Letters*, 19(2), pp. 1667-1691.
- Ragavendran, M. et al. (2017) 'Optimization of hybrid laser - TIG welding of 316LN steel using response surface methodology (RSM)', *Optics and Lasers in Engineering*, 94, pp. 27-36.
- Reddy, G.N. and VenkataRamana, M. (2018) 'Optimization Of Process Parameters In Welding Of Dissimilar Steels Using Robot TIG Welding', in *IOP Conference Series: Materials Science and Engineering. International Conference on Recent Advances in Materials, Mechanical and Civil Engineering*, Hyderabad, India: Trans Tech Publications, p. 012096.
- Samiuddin, M. et al. (2021) 'Investigation On The Process Parameters Of TIG-Welded Aluminum Alloy Through Mechanical And Microstructural Characterization', *Defence Technology*, 17(4), pp. 1234-1248.
- Shrivastava, S.P. et al. (2020) 'Investigation Of TIG Welding Parameters To Improve Strength', in *Materials Today: Proceedings. 10th International Conference of Materials Processing and Characterization*, Mathura, India: GLA University (10th International Conference of Materials Processing and Characterization), pp. 1897-1902.
- Singh, N.K. and Vijayakumar, Y. (2012) 'Application Of Taguchi Method For Optimization Of Resistance Spot Welding Of Austenitic Stainless Steel AISI 301L', *Innovative Systems Design and Engineering*, 3(10), p. 49.
- Sirohi, S. et al. (2023) 'Dissimilar Autogenous TIG Joint Of Alloy 617 And AISI 304H Steel For AUSC Application', *Heliyon*, 9(9), p. e19945.
- Siswanto, A.P. et al. (2022) 'Response Surface Methodology For Synthesis Of Bio-Jet Fuel From Waste Cooking Oil Using Agitated Ozone Treatment', in *Materials Today: Proceedings. 2nd International Conference on Chemical Engineering and Applied Sciences*, Semarang, Indonesia: Universitas Diponegoro (2nd International Conference on Chemical Engineering and Applied Sciences), pp. S346-S348.
- Sukarman et al. (2020) 'Analisis Pengaruh Radius Dies Terhadap Springback Logam Lembaran Stainless-Steel Pada Proses Bending Hidrolik V-Die', *Jurnal Teknologi*, 12(2), pp. 123-132.
- Sukarman, Shieddieque, A.D., et al. (2021) 'Optimization of Powder Coating Process Parameters in Mild Steel (SPCC-SD) To Improve Dry Film Thickness', *Journal of Applied Engineering Science*, 19(2), pp. 475-482.
- Sukarman, Abdulah, A., et al. (2021) 'Optimization Of The Resistance Spot Welding Process Of SECC-AF And SGCC Galvanized Steel Sheet Using The Taguchi Method', *SINERGI*, 25(3), pp. 319-328.
- Sukarman, Khoirudin, et al. (2023) 'Optimal Tensile-Shear Strength Of Galvanized/Mild Steel (SPCC-SD) Dissimilar Resistance Spot Welding Using Taguchi DOE', *Jurnal Teknologi*, 85(4), pp. 167-177.
- Sukarman, Triyono, et al. (2023) 'Tensile Shear Load In Resistance Spot Welding Of Dissimilar Metals: An Optimization Study Using Response Surface Methodology', *Mechanical Engineering for Society and Industry*, 3(2), pp. 66-77.
- Sukarman and Abdulah, A. (2020) 'Optimasi Single Response Proses Resistance Spot Welding Pada Penggabungan Baja Beda Material Menggunakan Metode Eksperimental Taguchi', *MULTITEK INDONESIA*, 14(2), pp. 69-79.
- Uijl, N.D. et al. (2012) 'Performance of Tensile Tested Resistance Spot and Laser Welded Joints at Various Angles', *Welding in the World*, 56(11), pp. 143-152.

- Venkatesan, G., Muthupandi, V. and Justine, J. (2017) 'Activated TIG Welding Of AISI 304L Using Mono-And Tri-Component Fluxes', *The International Journal of Advanced Manufacturing Technology*, 93(1), pp. 329-336.
- Vimal, K.E.K., Vinodh, S. and Raja, A. (2017) 'Optimization Of Process Parameters Of SMAW Process Using NN-FGRA From The Sustainability View Point', *Journal of Intelligent Manufacturing*, 28(6), pp. 1459-1480.
- Widyianto, A., Baskoro, A.S. and Kiswanto, G. (2022) 'Investigation on Weld Characteristic, Welding Position, Microstructure, and Mechanical Properties in Orbital Pulse Current Gas Tungsten Arc Welding of AISI 304L Stainless Steel Pipe', *IJTech - International Journal of Technology*, 13(3), pp. 473-483.
- Wirajaya, Y.M., Nugroho, N.Y. and Suwasono, B. (2021) 'Holding Time pada Sifat Fisik Pengelasan SMAW Baja ASTM-A36 melalui Uji Penetran', *Jurnal Jaring SainTek*, 3(2), pp. 45-50.
- Wu, H. et al. (2019) 'Research Advances In High-Energy TIG Arc Welding', *The International Journal of Advanced Manufacturing Technology*, 104(1), pp. 391-410.
- Xie, Y. et al. (2018) 'Characterization Of Keyhole Gas Tungsten Arc Welded AISI 430 Steel And Joint Performance Optimization', *The International Journal of Advanced Manufacturing Technology*, 99(1), pp. 347-361.